Growth and magnetic domain structure of ultrathin Fe films on Rh(001)

Jeannette Kemmer,[1,*] Stefan Wilfert,[1] Jens Kügel,[1] Tobias Mauerer,[1] Pin-Jui Hsu,[1,†] and Matthias Bode[1,2]

[1]*Physikalisches Institut, Lehrstuhl für Experimentelle Physik 2, Universität Würzburg, Am Hubland, 97074 Würzburg, Germany*

[2]*Wilhelm Conrad Röntgen-Research Center for Complex Material Systems (RCCM), Universität Würzburg, Am Hubland,*
D-97074 Würzburg, Germany

The growth and magnetic domain structure of ultrathin Fe films epitaxially grown on face-centered cubic (fcc) Rh(001) is investigated by spin-polarized scanning tunneling microscopy (SP-STM) at low temperatures ($T = 5.5$ K). Our results indicate that the cleaning procedure applied to the Rh(001) substrate plays an important role for the formation of a clean and well-ordered Fe film. The Fe monolayer exhibits an out-of-plane antiferromagnetic $c(2 \times 2)$ spin structure. Islands of the second Fe layer are found to be out-of-plane ferromagnetic. Coalescence of the double-layer islands results in the formation of larger domains, which extend over several hundred nanometers for a closed two layer film. Further increasing the Fe coverage leads to a reduction of the domain size and the formation of patterns that are reminiscent of stripe domains driven by the competition of surface/interface and shape anisotropy.

I. INTRODUCTION

Iron (Fe) is the prototypical ferromagnet. Its latin name, *ferrum*, is even used as a prefix for this class of spontaneously, permanently, and long-range ordered magnetic materials which are characterized by parallel moments. However, Fe is also a good example for the consequences of allotropy in metals as, besides the room temperature phase α-Fe with body-centered cubic (bcc) crystal structure, it also exists in the high-temperature phases of face-centered cubic (fcc) γ-, bcc δ-, and hexagonal close-packed (hcp) ϵ-Fe.

While the transition temperatures to these structural phases in pure bulk Fe are well above any potential magnetic ordering temperature, they can be stabilized in alloys or as thin films by epitaxial growth on suitable substrates. Interestingly, the magnetic properties of these stabilized allotropes differ distinctly from those of natural Fe. For example, fcc γ-Fe is antiferromagnetic, i.e., the magnetic moments alternately point in opposite directions and compensate each other on macroscopic length scales.

In fact, the magnetism of epitaxial Fe thin films on materials with an fcc crystal structure has intrigued scientists for decades. While early studies focused on Cu substrates, the magnetism of $3d$-transition metal films on $4d$- and $5d$-metal substrates has attracted considerable theoretical interest over the past decade [1–3]. Because of the spatial extension of $4d$ and $5d$ orbitals, the strong hybridization of film and substrate d electrons leads to some unusual properties, such as $c(2 \times 2)$ antiferromagnetic ground states [4], strongly enhanced interfacial magnetic moments in nonmagnetic substrates [5], and extremal values of the magnetocrystalline anisotropy [6].

Rhodium (Rh) is a $4d$-transition metal with a fcc crystal structure and a cubic lattice constant $a = 3.80$ Å [7]. The available literature on structural properties of Fe thin films on Rh(001) is rather inconsistent. Early experiments performed by low-energy electron diffraction (LEED) and Auger electron spectroscopy (AES) reported on the observation of pseudomorphic fcc films up to a film thickness of 30 Å [8]. A quantitative I-V LEED study found pseudomorphic layer-by-layer growth at room temperature for at least the initial three layers but a body-centered tetragonal (bct) structure at coverages larger than 7 atomic layers (AL) [9]. In contrast, for films deposited at a substrate temperature of 350 K another LEED study that was published almost simultaneously found an fcc film structure up to a coverage of 20 AL, even though the diffraction pattern showed a superstructure at 6 AL and became streaky at 8 AL [10].

Regarding the magnetic properties of Fe thin films on Rh(001), conflicting results have been published [11–15]. Early experiments performed by near-critical-angle reflection of polarized neutrons on films with a reported film thickness of 9 Å (though coated with a 50 Å Cu protection layer) found no in-plane ferromagnetic signal [11]. This observation was interpreted in terms of paramagnetic or antiferromagnetic Fe.

A spin-resolved photoemission spectroscopy and x-ray magnetic circular dichroism (XMCD) study by Hayashi and co-workers provided first evidence for ferromagnetism in Fe/Rh(001) [12]. It was found that a minimal film thickness of 3 AL is required for the occurrence of an in-plane XMCD signal. After magnetization along the $\langle 110 \rangle$ direction 4 and 8 AL thick Fe films exhibited a significant in-plane spin polarization of the photoelectrons. The magnetic moment linearly increases up to a film thickness of 6 AL and remains constant at even higher coverages. Subsequent XMCD data and theoretical band structure calculations explained the deferred onset of magnetic order by two magnetically "dead" layers at the Fe/Rh interface, which—according to Hayashi *et al.* in Refs. [13,14]—are caused by the above-mentioned face-centered tetragonal distortion of the Fe film. This atomic structure places the Fe at the interface to Rh(001) between ferromagnetic bcc and antiferromagnetic fcc Fe and eventually results in a nonmagnetic ground state.

---

*Corresponding author: jeannette.kemmer@physik.uni-wuerzburg.de

†Present address: Institute of Applied Physics and Interdisciplinary Nanoscience Center Hamburg, University of Hamburg, 20355 Hamburg, Germany.

In fact, theoretical investigations find an Fe magnetic structure which is strongly influenced by the underlying Rh substrate [1,2]. In agreement with the experimental observation of zero net magnetization [12–14], an in-plane $c(2 \times 2)$ antiferromagnetic ground state is calculated for the Fe monolayer [1,2]. However, theory predicts a ferromagnetic ground state for an Fe coverage of two atomic layers [1], although no magnetic signal could be detected down to $T = 97$ K [14]. While the Curie temperature of a 4.0 AL thick Fe film on Rh(001) amounts to approximately 530 K, a steep linear decrease has been observed towards thinner films. Linear extrapolation to an Fe coverage of 2.0 AL would suggest a Curie temperature of about 80 K [14]. This apparent discrepancy may be related to the film's tetragonal structure which leads to a competition between ferromagnetic bcc α- and the antiferromagnetism of fcc γ-Fe. It potentially results in a very low Curie temperature and/or excited magnetic states at relatively low excitation energies [1].

More recently a combined spin-polarized scanning tunneling microscopy (SP-STM) and magneto-optical Kerr effect (MOKE) study was performed by Takada *et al.* at a sample temperature $T = 5$ K [15], i.e., under conditions very similar to the study presented here. SP-STM data obtained on relatively defect-rich Fe monolayer films on Rh(001) were interpreted in terms of a complicated spin structure. Images taken with Fe- and Cr-coated tips were used to evaluate in-plane and out-of-plane contributions to the spin configuration. A noncollinear (2×3) spin configuration with a vanishing net magnetic moment was deduced. At coverages between 2.0 and 3.5 AL polar MOKE measurements showed a pronounced hysteresis indicating out-of-plane ferromagnetic films. At about 4 AL a rotation of the easy axis to in-plane was observed.

Here we investigate the structural and magnetic properties of thin Fe films on Rh(001) by SP-STM. Our results indicate that a thorough preparation procedure applied for cleaning the Rh substrate is a prerequisite towards high quality films. Namely, Rh(001) surfaces prepared solely by sputter-annealing cycles revealed numerous dislocation lines and pointlike defects which most likely originate from carbon (C) impurities. These crystal defects could be successfully removed by an oxygen treatment. Almost perfect layer-by-layer growth of Fe up to a coverage of two atomic layers appears on these substrates. At higher coverages island nucleation is observed before completion of a given layer. Edges of incomplete layers are preferentially oriented along the substrate's $\langle 110 \rangle$ directions. SP-STM data show that the Fe monolayer exhibits an out-of-plane antiferromagnetic $c(2 \times 2)$ spin structure. From the second layer on the Fe films exhibit out-of-plane ferromagnetic domains. While islands of the Fe double layer are mostly in a single domain state and exchange coupled to the surrounding antiferromagnetic monolayer, coalescence of islands leads to large domains. With increasing film thickness the evolution of a stripe domain phase can be observed.

II. EXPERIMENTAL SETUP AND PROCEDURES

A. Substrate preparation

For the preparation of clean Rh(001) surfaces various recipes have been applied. Although multiple repetitive sputter and annealing cycles are common to all experimental investigations, the specific parameters vary considerably across the literature [9–12,15,16]. With the exception of a single study, which used Ne [16], the sputtering was usually performed with Ar ions to remove surface contaminations. Reported annealing temperatures range from 900 [9,15] up to 1600 K [16] and durations from 5 min [12] up to 1 h [9].

Literature is even less consistent with respect to the question if any oxygen treatment is required to remove carbon from the Rh(001) surface. While the majority of studies abstain from the use of oxygen [9–12,15], Hwang *et al.* explicitly mention an oxygen treatment at a relatively low partial pressure $p_{ox} = 5 \times 10^{-9}$ mbar [16]. As we will report below, our experiments indicate that the surface carbon concentration of Rh(001) surfaces is indeed effectively reduced by the application of an oxygen treatment. In this context, Rh(001) surfaces behave similar to W(110) crystals, for which similar, essentially consistent observations have been made [17,18], even though some processing details regarding the optimal oxygen partial pressure and substrate temperatures are still the subject of debate. More importantly, the spatially resolved magnetic structures reported here, which could only be obtained on Rh(001) substrates cleaned by an oxygen treatment, deviate significantly from what has been observed previously on Fe films grown on untreated Rh(001) [15].

For the study presented here the Rh(001) substrate (MaTeck GmbH, average miscut about $0.1°$) was prepared in a dedicated chamber with a base pressure of $p \leqslant 1 \times 10^{-10}$ mbar. The initial treatment comprised of numerous cycles consisting of cold or hot Ar ion sputtering at a beam energy of $E_{ion} = 1$ keV and subsequent annealing on an *e*-beam heating stage at sample temperatures ranging from $T_{an} = 900$ K up to $T_{an} = 1300$ K. For example, Fig. 1(a) shows STM images of a Rh(001) surface that was prepared by Ar ion sputtering at $T_{sp} = 700$ K and annealing at $T_{an} = 960$ K. We would like to note that the appearance of this sample surface is very similar to what has been called "clean" Rh(001) by Takada *et al.* (cf. Fig. 2(a) in Ref. [15]). Although atomically flat terraces that are separated by monatomic step edges can clearly be recognized, several crystallographic defects that appear as bumps or short lines can already been seen in the overview image (left panel). In fact, the right image of Fig. 1(a), which was taken on a smaller scan range on an atomically flat area without step edges, reveals numerous pointlike defects. We speculate that they originate from carbon (C) impurities that— according to our experience—cannot be removed exclusively by sputter/annealing cycles.

Figure 1(b) shows a Rh(001) surface which was prepared by cycles that consist of about 10 min Ar ion sputtering at room temperature ($p_{Ar} = 5 \times 10^{-6}$ mbar, $E_{ion} = 1$ keV), followed by 150 s annealing at $T_{an} = 1300$ K in an oxygen atmosphere, and a final flash (duration about 30 s) without oxygen at the same temperature. The oxygen was introduced through a nozzle that was positioned about 2–3 cm above the Rh(001) surface. While we cannot quantify the oxygen partial pressure at the location of the sample, vacuum gauge and quadrupole mass spectrometer measurements indicate a chamber pressure $p = 1 \times 10^{-8}$ mbar and an effective purity better than 99.95%, respectively. As can be seen in the overview STM image in the left panel of Fig. 1(b) this cleaning procedure results in a
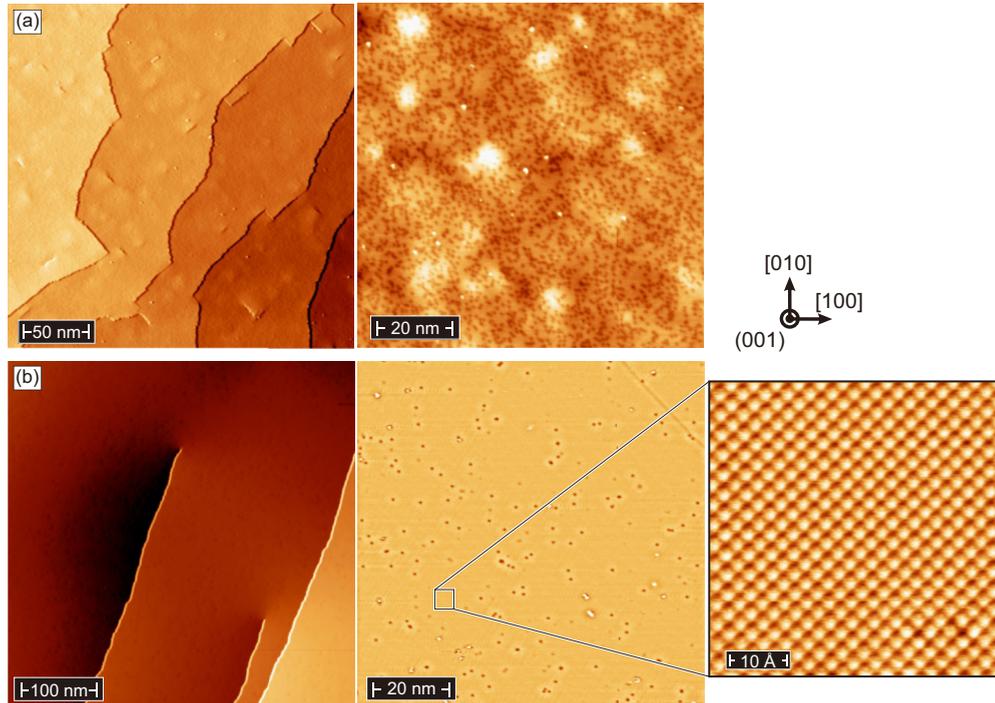
FIG. 1. (Color online) Topographic STM images of the bare Rh(001) surface as prepared by different procedures: (a) by sputtering and annealing and (b) with additional oxygen treatment (see text for details). While the surface contains numerous defects in (a), which probably originate from carbon, a very low defect density is observed in (b). Scan parameters: $U = +1$ V, $I = 200$ pA (atomic resolution: $U = +2$ mV, $I = 10$ nA).

much smoother surface without any bumps or linear defects. Furthermore, the higher magnification image in the right panel of Fig. 1(b) shows that the density of point defects is reduced to about 200 on a 100 nm × 100 nm scan frame, equivalent to an impurity density below 0.2%. On such a surface atomic resolution can be achieved, as shown in the inset of Fig. 1(b).

B. Fe film deposition

Fe films were grown in the preparation chamber with a base pressure $p < 1 \times 10^{-10}$ mbar using a commercial e-beam evaporator loaded with an Fe rod (2 mm diameter). After extended degassing the background pressure during Fe deposition did not exceed $p = 3 \times 10^{-10}$ mbar. Fe layer thicknesses are given in equivalents of pseudomorphic atomic layers (AL) on Rh(001), i.e., 13.82 atoms/nm^2. The deposition rate was determined by submonolayer growth on Rh(001) and approximately amounts to 1 AL/min. The growth was performed while the Rh(001) substrate was cooling down from the final flash at a temperature of about 315 K. As compared to room temperature deposition used in Ref. [15], to our experience the slightly enhanced substrate temperature results in a better layer-by-layer growth (data not shown here). For the detailed analysis of the thickness-dependent magnetic domain structure of Fe films on Rh(001) presented below higher growth temperatures were avoided because the formation of a surface alloy and/or interdiffusion cannot be excluded.

C. Spin-polarized scanning tunneling microscopy (SP-STM)

STM experiments were performed in a UHV chamber with a base pressure of $p \leqslant 5 \times 10^{-11}$ mbar. After preparation,

the sample was immediately transferred from the preparation chamber into a home-built low-temperature scanning tunneling microscope (LT-STM) (operation temperature $T = 5.5$ K). For topographic images, the LT-STM was operated in the constant-current mode with the bias voltage (U) applied to the sample.

We used electrochemically etched polycrystalline W tips which can be transferred through the UHV system by means of a shuttle and inserted into the STM with a wobble stick. For spin-resolved STM measurements the tips were flashed by electron bombardment, then coated with an Fe or Cr film at room temperature, and eventually annealed to about $T_{\mathrm{an}} = 600$ K for 4 min. Cr film thickness was calibrated by submonolayer deposition on a W(110) substrate [19]. Using these magnetically coated probe tips spin-sensitive differential conductance (dI/dU) maps were acquired by lock-in technique with a small voltage modulation U_{mod} (typically of the order of one-tenth of the applied bias voltage) added to the tunneling voltage (frequency $f = 5.777$ kHz).

III. RESULTS AND DISCUSSION

A. Fe monolayer and second layer islands on Rh(001)

Our experiments indicate that the first atomic layer of Fe on Rh(001) almost perfectly closes before nucleation of the second layer. For example, Fig. 2(a) shows the large-scale topography of a 1.1 AL Fe film on Rh(001). With the exception of a few tiny holes, which amount to less than 1% of the total surface area, the first Fe layer on Rh(001) is completed. Fe material in excess of one pseudomorphic layer has formed
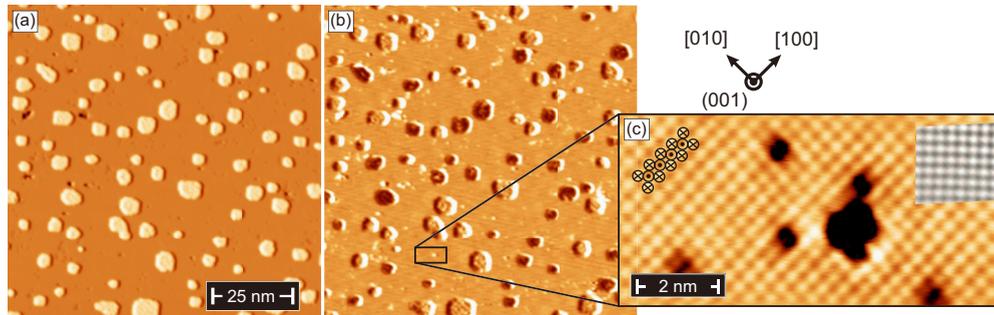
FIG. 2. (Color online) (a) Large-scale topographic STM image of 1.1 AL Fe/Rh(001) and (b) spin-resolved dI/dU map obtained with a Cr-coated W tip sensitive to the out-of-plane direction. A two-stage magnetic contrast can be recognized in (b) indicating the perpendicular easy axis of the double layer. (c) Atomically resolved SP-STM topography (constant-current image) measured on the Fe monolayer on Rh(001). It reveals an out-of-plane antiferromagnetic $c(2 \times 2)$ spin structure which is schematically represented in the upper left corner. The gray-scaled inset shows a corresponding spin-averaged measurement performed with a nonmagnetic tip. Note the different size and orientation of the square lattice. Scan parameters: $U = -1$ V, $I = 200$ pA (atomic resolution: $U = +3$ mV, $I = 80$ nA).

islands of the second layer. Although somewhat rounded, a preferential orientation of the island edges along the substrate's $\langle 110 \rangle$ directions can clearly be recognized. The typical lateral size amounts to edge length ranging between 5 and 10 nm. No indication for the nucleation of the third Fe layer could be found at this coverage.

Figure 2(b) displays a dI/dU map which was recorded simultaneously with Fig. 2(a). Since a Cr-coated W tip was used this SP-STM measurement is sensitive to the out-of-plane direction of the magnetization. While the monolayer appears uniform at this scale, a clear dark/bright contrast can be recognized on the double-layer islands [20]. This observation indicates a perpendicular easy axis for the second Fe layer on Rh(001), a finding corroborated by experiments that will be presented further below. The higher magnification image shown in Fig. 2(c) taken in between the double-layer islands reveals that the Fe monolayer on Rh(001) possesses an out-of-plane $c(2 \times 2)$ spin structure, similar to the one observed for the monolayer of Fe/W(001) [4].

As shown by comparison with an atomic resolution image obtained on a different but equivalent sample with a nonmagnetic W tip [see inset of Fig. 2(c)], the magnetic $c(2 \times 2)$ structure is characterized by a lattice that is rotated by 45° with respect to the spin-averaged atomic lattice and exhibits a $\sqrt{2}$ larger lattice spacing. It has been shown theoretically that—in particular for chemically homogeneous surfaces—atomic-scale SP-STM images are often dominated by the magnetic structure and show little evidence of the underlying structural lattice [21].

B. Coalescence, growth, and magnetic domain structure of Fe/Rh(001)

In the following we will present SP-STM data obtained with an Fe-coated probe tip the magnetization direction of which unintentionally changed in between two scans. Although any experimentalist performing magnetically sensitive scanning probe studies is usually anxious to avoid such tip changes, here it provides us with a better understanding of the magnetic domain and domain wall structure of Fe films on Rh(001) at coverages beyond 2.0 AL.

Figure 3(a) shows a topographic STM image of a 2.3 AL Fe film on Rh(001). Note that the film was grown at a substrate
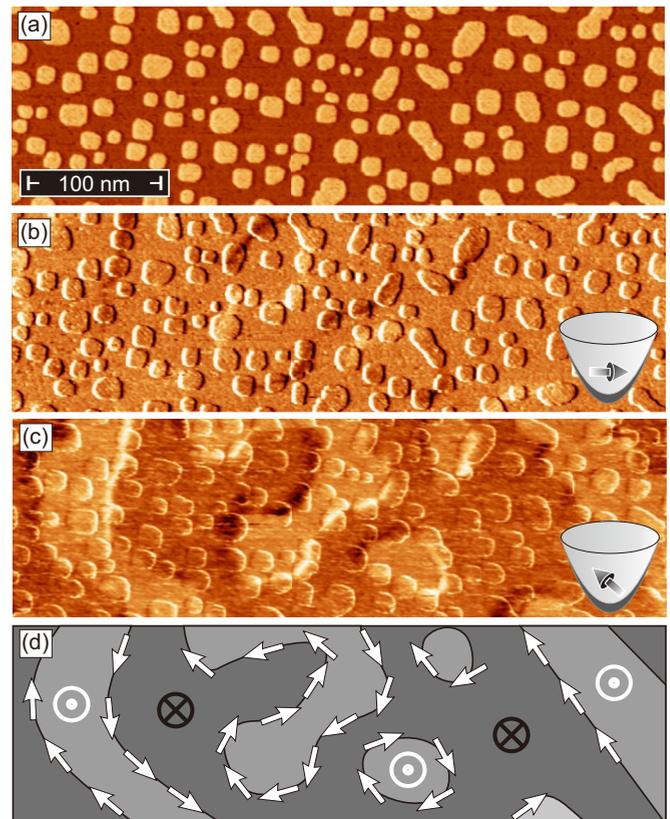

FIG. 3. (Color online) (a) STM topograph of a 2.3 AL Fe film on Rh(001) showing islands with a local coverage of 3 AL on a closed double layer. (b) Spin-resolved STM image obtained simultaneously with (a) using an Fe-coated tip with in-plane sensitivity. Dark and bright domain walls running predominantly across third layer islands can be recognized. (c) Subsequent spin-resolved STM image taken at the same location with the same tip as (a) and (b) after an unintentional modification occurred to the tip resulting in a canted magnetization direction. (d) Schematics of the surface magnetic domain and Bloch domain wall structure. Note that Néel walls or oppositely magnetized domains and/or domain walls would also be consistent with the experimental data presented in (b) and (c).

temperature of 340 K, i.e., slightly higher than the results which will be presented further below. As a result the double layer is perfectly closed and comparably large islands with a local coverage of three atomic layers can be recognized. Since the magnetization of the tip apex of Fe-coated tips is usually oriented perpendicular to the tip axis [22], i.e., parallel with respect to the sample surface, no contrast is expected from the domain of an out-of-plane magnetized film. In agreement with this expectation, the usual dark/bright contrast is absent in the dI/dU map presented in Fig. 3(b). However, narrow bright and dark lines can clearly be recognized which probably originate from in-plane magnetized domain walls located between the differently oriented out-of-plane domains.

This interpretation is corroborated by the following dI/dU map [Fig. 3(c)] which was taken after a spontaneous and uncontrolled tip change had occurred, possibly caused by a dipolar, i.e., stray-field-mediated interaction between tip and sample. Now both a domain and a domain wall contrast is obtained, indicating that the modified tip exhibits a canted magnetization direction. Note that—compared to Fig. 3(b)—in Fig. 3(c) an inverted contrast is obtained within the domain walls, indicating an opposite in-plane component.

Interestingly, Fig. 3(c) also reveals that for any bright domain the dark (bright) segment of the surrounding domain wall appears on the upper left (lower right). This observation indicates that the sense of rotation of the domain walls is always the same, or—in other words—that the domain walls are chiral with a unique sense of rotation. Therefore, the spin structure of the Fe double layer on Rh(001) can be regarded as a Skyrmion [23–25] with a very long wavelength. Potentially this chirality is caused by the spin-orbit coupling-induced Dzyaloshinskii-Moriya interaction (DMI) [25].

Based on the information contained in the images displayed in Figs. 3(b) and 3(c) we can generate a schematic map of the domain pattern of the surface area under investigation. It is presented in Fig. 3(d). While we are convinced that this scheme gives an overall correct impression of the magnetic configuration, we would like to emphasize that similar patterns with oppositely magnetized domains and/or domain walls would also be consistent with our experimental results. Furthermore, Fig. 3(d) shows domain walls where the magnetization direction rotates within the wall plane, i.e., Bloch walls, although Néel walls expected for Skyrmions caused by the DMI [26] are also consistent with our data. In order to distinguish these two scenarios a better control over the tip magnetization would be required, as it may be achieved by an external field that is larger than the coercive field of the tip but still low enough to maintain the sample's magnetic domain structure in its nascent state [27]. Unfortunately such an external field capability was not available in the current setup.

In order to avoid any impact of the stray field of the probe tips [28] and to match the requirements implied by a perpendicularly magnetized film we have employed out-of-plane sensitive Cr-coated probe tips for the following coverage-dependent study. Figure 4 shows an overview over the growth (left column), a topographic STM image at higher magnification (middle), and the magnetic domain structure as obtained by SP-STM (right column) of Fe films on Rh(001) in the coverage range between 1.7 and 3.4 AL. At an Fe coverage of 1.7 AL the double-layer islands coalesce and

form networks [left panel of Fig. 4(a)]. In spite of the fact that the double layer is already 70% filled, the inset of Fig. 4(a) shows only very few extremely tiny clusters of third layer nuclei. Obviously coalescence strongly influences the magnetic domain structure observed on double layer, as can be recognized in the SP-STM data displayed in the right panel of Fig. 4(a). While the Fe double-layer islands which were well separated at lower coverage in Fig. 2(b) could be considered as single domain particles, the formation of a closed network of second layer patches leads to irregularly shaped, but uniformly magnetized areas, i.e., domains, with typical lateral dimensions of several tens of nanometers. Boundaries between domains with opposite magnetization directions are preferentially found at locations where the second Fe layer is discontinuous or at structural constrictions, thereby minimizing the domain wall energy [29–31].

The left panel of Fig. 4(b) shows the topography of an Fe film on Rh(001) at a thickness of 2.1 AL. At this coverage the second Fe layer is essentially perfectly closed with only a few holes with monolayer coverage and some third layer islands on top. These third layer islands are shown at higher magnification in the middle panel of Fig. 4(b), with edges along ⟨110⟩ directions and a typical size of less than 10 nm. Again, the drastically changed topology of the perpendicularly magnetized second Fe layer has dramatic consequences for the domain structure we observe by SP-STM in the right panel of Fig. 4(b). Extended perpendicularly magnetized domains were found with typical lateral dimensions of (300 ± 100) nm. Domain walls often, but not strictly, run along bunched step edges, as can be seen in the central region of the SP-STM image shown in Fig. 4(b). In contrast, the islands do not appear to strongly influence the position of domain walls which were found to be about 4 nm wide in 2 AL thick films (not shown here).

As can be seen in the left and middle panel of Fig. 4(c) the growth of Fe/Rh(001) somewhat deviates from a layer-by-layer growth mode after completion of the second layer. Although the coverage amounts to 2.6 AL only, nucleation of the fourth and fifth layer on islands of the third layer can clearly be recognized. At all coverages the island edges are oriented along ⟨110⟩ directions. Also the magnetic domain structure shows some significant changes. Namely, the domains become smaller [about (100 ± 30) nm wide] and are irregularly shaped. Although we cannot present large scale images because of the limited scan range of our microscope, the impression we got from images similar to the one presented in the right panel of Fig. 4(c) is that the domains tend to form a pattern that very much resembles the slightly meandering stripe domains observed on Fe/Ni/Cu(001) samples (cf. Fig. 1(a) in Ref. [32]).

At the highest coverage investigated in this study, i.e., 3.4 AL Fe/Rh(001), the third layer is almost closed, leaving only narrow trenches with a local coverage of 2 AL behind [left panel of Fig. 4(d)]. Now, even a few sixth layer islands can be found. Although the spin-resolved measurement shown in the right panel of Fig. 4(d) were plagued by a mixed magnetic contrast showing a very significant contribution from in-plane components of the magnetization, a further reduction of the domain size as compared to the data of Fig. 4(c) can clearly be recognized.
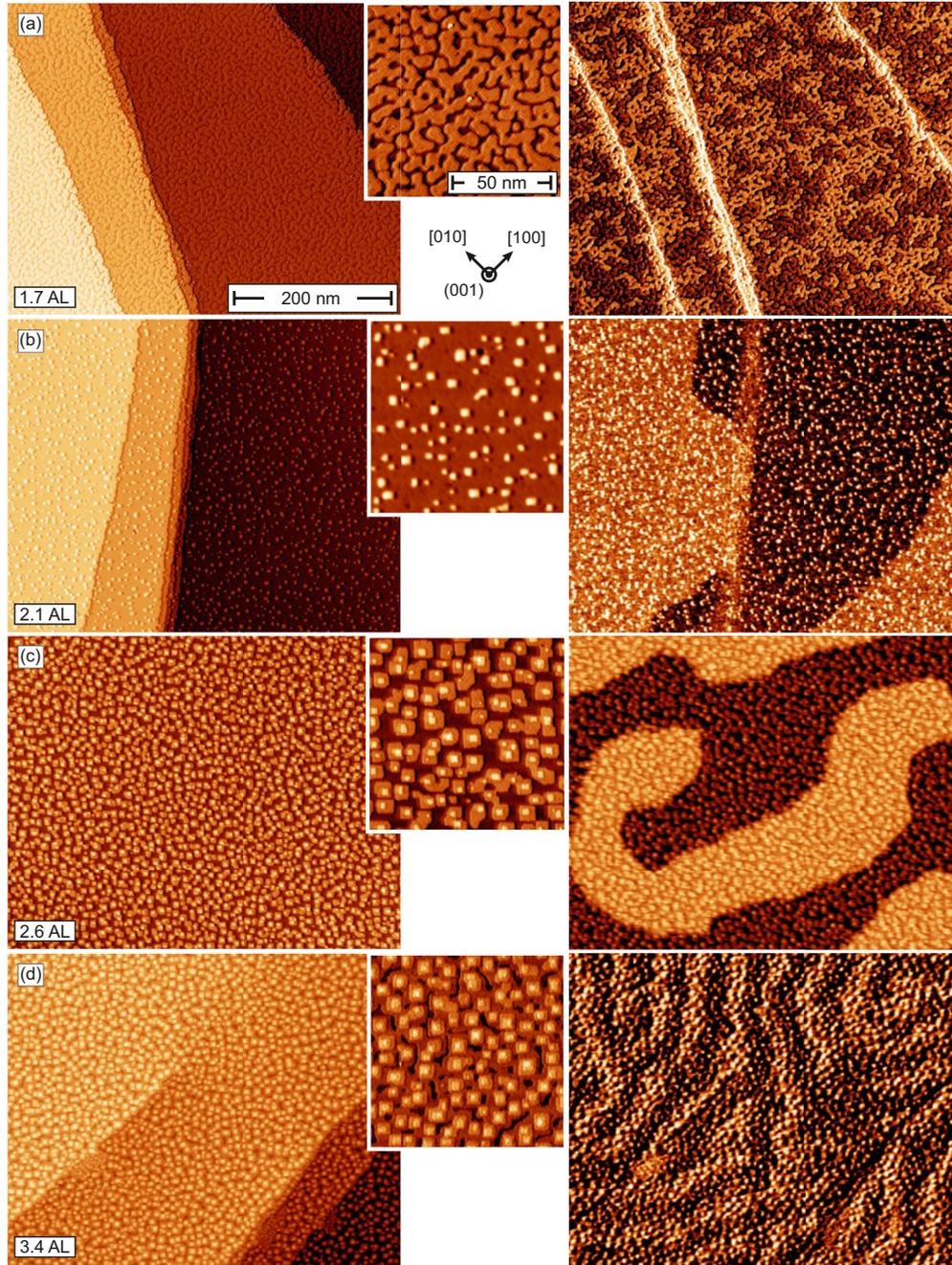
FIG. 4. (Color online) Coverage-dependent topographic STM images showing an overview (left panel) and a zoomed-in (middle) along with the magnetic domain structure as obtained by SP-STM (right) of Fe films on Rh(001): (a) 1.7 AL (scan parameters: $U = -0.6$ V, $I = 1.5$ nA), (b) 2.1 AL ($U = -0.7$ V, $I = 3.0$ nA), (c) 2.6 AL ($U = -0.7$ V, $I = 1.5$ nA), and (d) 3.4 AL ($U = -0.5$ V, $I = 2.5$ nA).

C. Discussion of the domain structure

The formation of stripe domains in perpendicularly magnetized thin films as well as the strong reduction of the domain size with increasing film thickness is well known [33] and has been theoretically predicted [34], modeled [35–39], and experimentally observed in multiple sample systems [32,40–43]. The driving mechanism is the competition of different terms that contribute to total magnetic energy: (i) the magnetocrystalline anisotropy energy K_s, which in many thin films is governed by surface and interface contributions and often favors an out-of-plane magnetization of the film [44],

(ii) the energy associated with the stray field (also called dipolar energy), and (iii) the domain wall energy that increases as the domain width decreases [33]. Since the dipolar energy is acting on relatively large length scales the stray field generated outside the sample can be significantly reduced by flux closure between domains with alternating up and down magnetization [33]. The equilibrium configuration is characterized by a minimal total magnetic energy. Eventually, at a critical thickness t_c, the perpendicular magnetocrystalline anisotropy cancels the in-plane magnetic shape anisotropy and spin reorientation transition (SRT) takes place, where the
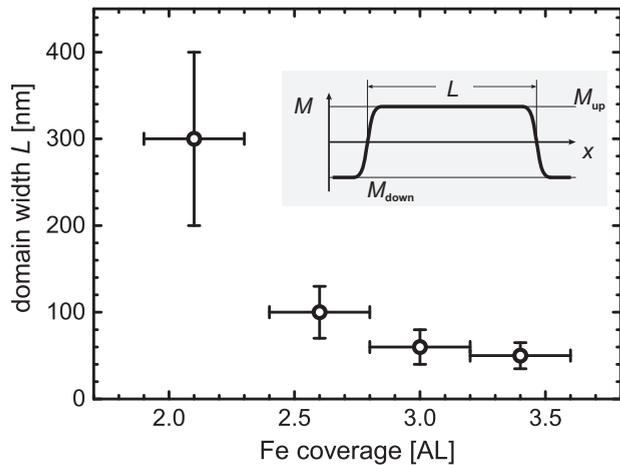
FIG. 5. Coverage dependence of the stripe domain width L versus coverage observed for Fe/Rh(001).

easy magnetization axis changes from perpendicular at low thickness to in-plane with respect to the film plane.

In fact, the domain structure we observed in the thickness range between 2 and 3.4 AL Fe/Rh(001) is perfectly consistent with the MOKE data presented by Takada *et al.* (cf. Fig. 3 in Ref. [15]). In short, these data show hysteresis in polar Kerr loops between 2 and 3.5 AL Fe/Rh(001), whereby the coercive field continuously decreases with increasing film thickness. At a coverage of 4.0 AL a significant hysteresis of the in-plane magnetization was observed by planar MOKE, indicating an SRT between 3.5 and 4.0 AL Fe/Rh(001) [15]. At this point the ratio of K_s to the dipolar energy that defines the parameter f introduced in Yafet and Gyorgy's original publication [34] reaches the threshold value f_{min}. Further increasing the film thickness leads to a situation where the energy required for the formation of domain walls between the stripe domains becomes larger than the energy gained by the reduction of the stray field.

A more quantitative evaluation reveals some unexpected observations. For example, a similar behavior of the domain pattern has been reported in Fe films that were exchange coupled to a 5 AL Ni/Cu(001) sample [39,43]. Also in this case, a drastic reduction of the domain width with increasing Fe thickness was observed. The zero field minimum stripe domain width L_{min} at the spin reorientation transition ($t_c = 2.7$ AL) was experimentally determined to about 0.2–0.3 μm. This value agrees well with model calculations that consider the magnetic exchange interaction, the magnetocrystalline anisotropy, and dipolar interactions, leading to $L_{min} = 2.27 J\pi^2/\Omega_L = 0.33\ \mu$m, where J is the nearest-neighbor

exchange interaction and Ω_L is the long-range part of the dipolar interaction [43]. In the case of Fe/Rh(001) the experimentally obtained values are about an order of magnitude smaller, as can be seen in the plot of the stripe domain width L versus Fe coverage in Fig. 5. This is rather surprising since—under assumption that the actual parameters for J and Ω_L are very similar to the Fe/5 AL Ni/Cu(001) case—one would expect a very similar minimum stripe domain width L_{min} at the spin reorientation transition.

The apparent discrepancy might be explained by the above-mentioned consequences of the film's tetragonal distortion [1]. The competition between ferromagnetic bcc α- and the antiferromagnetism of fcc γ-Fe may lead to very low values of the effective nearest-neighbor exchange interaction J, at least for the layers which are in direct contact with the substrate or very close to the interface. Besides the unexpectedly narrow domain width this scenario could also explain the very low Curie temperature of the Fe double layer on Rh(001). Further research on this interesting topic and the potential influence of low-energy excitations or competing phase transitions will be required to better understand these extraordinary properties.

IV. SUMMARY

In summary, we have studied the growth and magnetic domains structure of ultrathin Fe films on Rh(001) by spin-polarized scanning tunneling microscopy (SP-STM). According to our experience clean Rh(001) surfaces can only be obtained by a combination of sputter and annealing cycles with occasional oxygen treatments. Under these conditions the first two atomic layers of Fe exhibit an almost perfect layer-by-layer growth. At coverages between 2.0 and 3.5 AL island nucleation is observed. In contrast to earlier SP-STM data but in agreement with theoretical predictions we find an out-of-plane antiferromagnetic $c(2 \times 2)$ spin structure for the monolayer. Out-of-plane ferromagnetic domains are observed for local coverages of 2 and 3 AL. With increasing film thickness the evolution of a stripe domain phase can be observed. Quantitative evaluation reveals that the results obtained for Fe/Rh(001) are not constant with simple models using material parameters of fcc Fe. The unexpectedly narrow domain width is potentially caused by an extremely low value of the effective nearest-neighbor exchange interaction J at and close to the Fe–Rh interface, which would also explain the unusually low Curie temperature found for the Fe double layer on Rh(001) in earlier publications.

[1] D. Spišák and J. Hafner, Phys. Rev. B **73**, 155428 (2006).

[2] A. Al-Zubi, G. Bihlmayer, and S. Blügel, Phys. Rev. B **83**, 024407 (2011).

[3] A. Al-Zubi, G. Bihlmayer, and S. Blügel, Phys. Status Solidi (b) **248**, 2242 (2011).

[4] A. Kubetzka, P. Ferriani, M. Bode, S. Heinze, G. Bihlmayer, K. von Bergmann, O. Pietzsch, S. Blügel, and R. Wiesendanger, Phys. Rev. Lett. **94**, 087204 (2005).

[5] F. Wilhelm, P. Poulopoulos, H. Wende, A. Scherz, K. Baberschke, M. Angelakeris, N. K. Flevaris, and A. Rogalev, Phys. Rev. Lett. **87**, 207202 (2001).

[6] G. van der Laan, J. Phys.: Condens. Matter **10**, 3239 (1998).

[7] J. W. Ablaster, Platinum Met. Rev. **41**, 184 (1997).

[8] A. A. Hezaveh, G. Jennings, D. Pescia, R. F. Willis, K. Prince, M. Surman, and A. Bradshaw, Solid State Commun. **57**, 329 (1986).

[9] A. M. Begley, S. K. Kim, F. Jona, and P. M. Marcus, Phys. Rev. B **48**, 1786 (1993).

[10] C. Egawa, Y. Tezuka, S. Oki, and Y. Murata, Surf. Sci. **283**, 338 (1993).

[11] J. A. C. Bland, D. Pescia, and R. F. Willis, Phys. Rev. Lett. **58**, 1244 (1987).

[12] K. Hayashi, M. Sawada, A. Harasawa, A. Kimura, and A. Kakizaki, Phys. Rev. B **64**, 054417 (2001).

[13] K. Hayashi, M. Sawada, H. Yamagami, A. Kimura, and A. Kakizaki, Phys. B: Condens. Matter **351**, 324 (2004).

[14] K. Hayashi, M. Sawada, H. Yamagami, A. Kimura, and A. Kakizaki, J. Phys. Soc. Jpn. **73**, 2551 (2004).

[15] M. Takada, P. L. Gastelois, M. Przybylski, and J. Kirschner, J. Magn. Magn. Mater. **329**, 95 (2013).

[16] C. Hwang, A. K. Swan, and S. C. Hong, Phys. Rev. B **60**, 14429 (1999).

[17] M. Bode, S. Krause, L. Berbil-Bautista, S. Heinze, and R. Wiesendanger, Surf. Sci. **601**, 3308 (2007).

[18] K. Zakeri, T. Peixoto, Y. Zhang, J. Prokop, and J. Kirschner, Surf. Sci. **604**, L1 (2010).

[19] B. Santos, J. M. Puerta, J. I. Cerda, R. Stumpf, K. von Bergmann, R. Wiesendanger, M. Bode, K. F. McCarty, and J. de la Figuera, New J. Phys. **10**, 013005 (2008).

[20] M. Bode, A. Kubetzka, K. von Bergmann, O. Pietzsch, and R. Wiesendanger, Microsc. Res. Technique **66**, 117 (2005).

[21] S. Heinze, Appl. Phys. A **85**, 407 (2006).

[22] M. Bode, Rep. Prog. Phys. **66**, 523 (2003).

[23] U. K. Rößler, A. N. Bogdanov, and C. Pfleiderer, Nature (London) **442**, 797 (2006).

[24] S. Mühlbauer, B. Binz, F. Jonietz, C. Pfleiderer, A. Rosch, A. Neubauer, R. Georgii, and P. Böni, Science **323**, 915 (2009).

[25] A. Fert, V. Cros, and J. Sampaio, Nat. Nano. **8**, 152 (2013).

[26] M. Heide, G. Bihlmayer, and S. Blügel, Phys. Rev. B **78**, 140403(R) (2008).

[27] S. Meckler, N. Mikuszeit, A. Preßler, E. Y. Vedmedenko, O. Pietzsch, and R. Wiesendanger, Phys. Rev. Lett. **103**, 157201 (2009).

[28] A. Kubetzka, M. Bode, O. Pietzsch, and R. Wiesendanger, Phys. Rev. Lett. **88**, 057201 (2002).

[29] P. Bruno, Phys. Rev. Lett. **83**, 2425 (1999).

[30] O. Pietzsch, A. Kubetzka, M. Bode, and R. Wiesendanger, Phys. Rev. Lett. **84**, 5212 (2000).

[31] N. Kazantseva, R. Wieser, and U. Nowak, Phys. Rev. Lett. **94**, 037206 (2005).

[32] J. Choi, J. Wu, C. Won, Y. Z. Wu, A. Scholl, A. Doran, T. Owens, and Z. Q. Qiu, Phys. Rev. Lett. **98**, 207205 (2007).

[33] A. Hubert and R. Schäfer, *Magnetic Domains* (Springer, Berlin, 2000).

[34] Y. Yafet and E. M. Gyorgy, Phys. Rev. B **38**, 9145 (1988).

[35] K.-O. Ng and D. Vanderbilt, Phys. Rev. B **52**, 2177 (1995).

[36] A. B. MacIsaac, K. De'Bell, and J. P. Whitehead, Phys. Rev. Lett. **80**, 616 (1998).

[37] E. Y. Vedmedenko, H. P. Oepen, A. Ghazali, J. C. S. Lévy, and J. Kirschner, Phys. Rev. Lett. **84**, 5884 (2000).

[38] K. De'Bell, A. B. MacIsaac, and J. P. Whitehead, Rev. Mod. Phys. **72**, 225 (2000).

[39] C. Won, Y. Z. Wu, J. Choi, W. Kim, A. Scholl, A. Doran, T. Owens, J. Wu, X. F. Jin, H. W. Zhao, and Z. Q. Qiu, Phys. Rev. B **71**, 224429 (2005).

[40] R. Allenspach and A. Bischof, Phys. Rev. Lett. **69**, 3385 (1992).

[41] M. Speckmann, H. P. Oepen, and H. Ibach, Phys. Rev. Lett. **75**, 2035 (1995).

[42] O. Portmann, A. Vaterlaus, and D. Pescia, Nature (London) **422**, 701 (2003).

[43] Y. Z. Wu, C. Won, A. Scholl, A. Doran, H. W. Zhao, X. F. Jin, and Z. Q. Qiu, Phys. Rev. Lett. **93**, 117205 (2004).

[44] U. Gradmann, J. Magn. Magn. Mater. **100**, 481 (1991).